Journal of Visualization, Vol. 7, No. 4 (2004) 331-340

Warm Ocean Water Intrusion into Kagoshima Bay

Kohno, J.[*1], Hosotani, K.[*1], Ono, Y.[*2] and Kikukawa, H.[*2]

*1 Kagoshima Environmental Research and Service, Nanatsushima 1-1-5, Kagoshima 891-0132, Japan.
E-mail: hosotani@kagoshima-env.or.jp
*2 Department of Environmental and Information Sciences, Faculty of Fisheries, Kagoshima University, Shimoarata 4-50-20, Kagoshima 890-0056, Japan.
E-mail: kikukawa@fish.kagoshima-u.ac.jp

Received 15 August 2003
Revised 10 June 2004

Abstract : From the field observations and the buoy robot data, the warm ocean water is known to intrude into Kagoshima Bay intermittently in winter. We first visualize these phenomena using some satellite thermal infrared images. Then the numerical analysis is performed employing a multi-level finite difference method (FDM). It is found from the numerical analysis that the intrusion occurs when the warm water comes into touch with the bay water at the mouth of the bay. The calculated warm water distribution in the bay is similar to the satellite images and the velocity of the intrusion is the same order with the ones estimated by the buoy robot data and the satellite images. The intrusion occurs even without the tidal effect, the role of the tide is only to rectify some warm water distribution in the bay.

Keywords : Kagoshima Bay, Intrusion, Warm water, Satellite image, Numerical simulation.

1. Introduction

Kagoshima Bay is located in the southern end of Kyusyu, Japan (Fig. 1). It is long in south to north with the length of about 75 km. There is a sill with the depth of about 100m at the mouth opened to the south. Close to the mouth of the bay the Kuroshio Current flows. The bay has two deep basins connected by Sakurajima channel of about 2km wide and 40m deep. Caused by the semi-enclosed shape of the bay, the contamination of the bay water brings a serious environmental problem.

The exchange of water in Kagoshima Bay takes place mainly in winter by density current (Takahashi, 1981; Kikukawa et al., 1997). However, the intermittent inflow of the open-ocean water is observed by Sakurai (1983), which may also play an important role in the purgation of the bay water.

Intrusion of the warm ocean water into Kagoshima Bay in winter is also collaborated by the buoy robot data and the thermal infrared satellite images

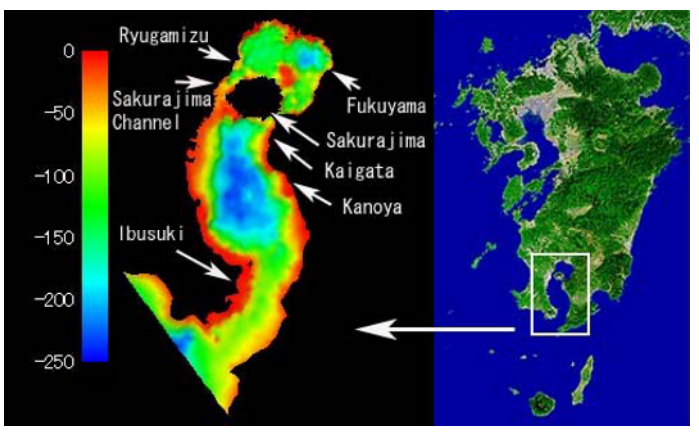

Fig. 1. Bottom topography of Kagoshima Bay.

(Ohtani et al., 1998).

In this paper, we focus on the warm water intrusion into Kagoshima Bay in winter. First the buoy robot data and then the satellite images are shown, for the purpose to visualize the ocean water intrusion. Next we try to analyze the phenomena by a numerical simulation.

2. Buoy Robot Data and Satellite Images

From 1992 to 1996, buoy robots were set up at the off shores of Kanoya, Kaigata, Ryugamizu and Fukuyama shown in Fig. 1, for the purpose to acquire data of the water temperature, the electrical conductivity and the dissolved oxygen up to 10m deep in fish farms. The hourly data were sent to the Kagoshima Prefectural Experimental Station of Fisheries by radio wave.

Figure 2 shows the water temperature at 1m deep in 1995, which is averaged over 24 hours to avoid the needless complexity. We can see from Fig. 2 that at Kanoya and Kaigata located in the south basin, the abnormal ascents exist from December to April, while at Ryugamizu and Fukuyama in the north basin, the temperature changes smoothly in winter. The temperatures at 5m and 10m deep behave almost equally as the one at 1m deep.

Figure 3 shows the water temperature at 1m deep at Kanoya and Kaigata from Jan. 15 to 31 in 1994. The ascents of the water temperature are seen from Jan. 18 to 22 and from Jan. 25 to 29 at Kanoya, but only Jan. 26 to 30 at Kaigata, which is located about 8km north from Kanoya.

The abnormal ascents of the water temperature in winter might be the evidence of the ocean water intrusion into the bay. However, the definite proofs are given by the satellite images.

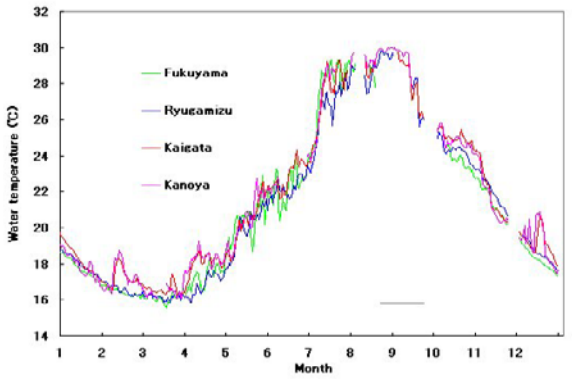

Fig. 2. Water temperature at 1m deep in 1995.

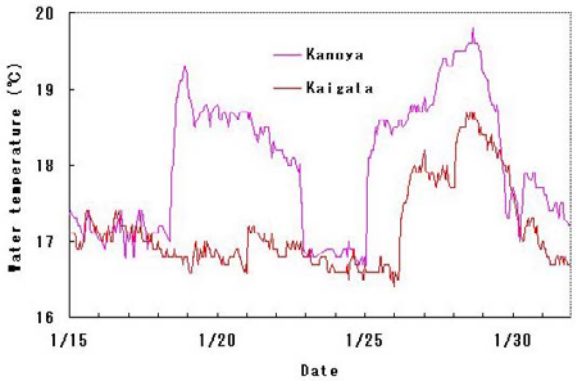

Fig. 3. Water temperature at 1m deep from Jan. 15 to 31, 1994.

Figure 4 is the thermal infrared images of Landsat5 and 7. These images clearly show that the warm ocean water intrudes into the south basin along its east coast, and does not go into the north basin. There exist only three Landsat images of the ocean water intrusion for these 20 years, owing to the fact that the recurrence of Landsat is 17days.

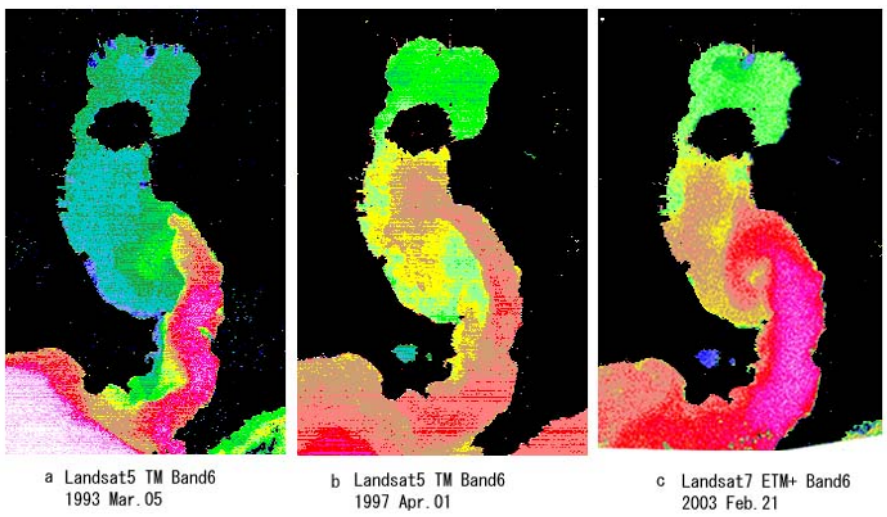

Fig. 4. Band6 images of Landsat5 TM and Landsat7 ETM+. Warm (cool) hues represent warm (cool) water.

At Kagoshima Univ., NOAA data have been received since April 1997. We can receive at least four NOAA data every day with the resolution (IFOV: instantaneous field of view) of 1.1km, which is not enough to see the detailed structure in the bay. Thus the images are 8 times enlarged using the linear interpolation, so that the apparent resolution becomes 137.5m. Figure 5 shows the 8 times enlarged NOAA images representing 3 examples of the warm water intrusion. The speed of warm water inflow is estimated to be about 7 to 10cm/s.

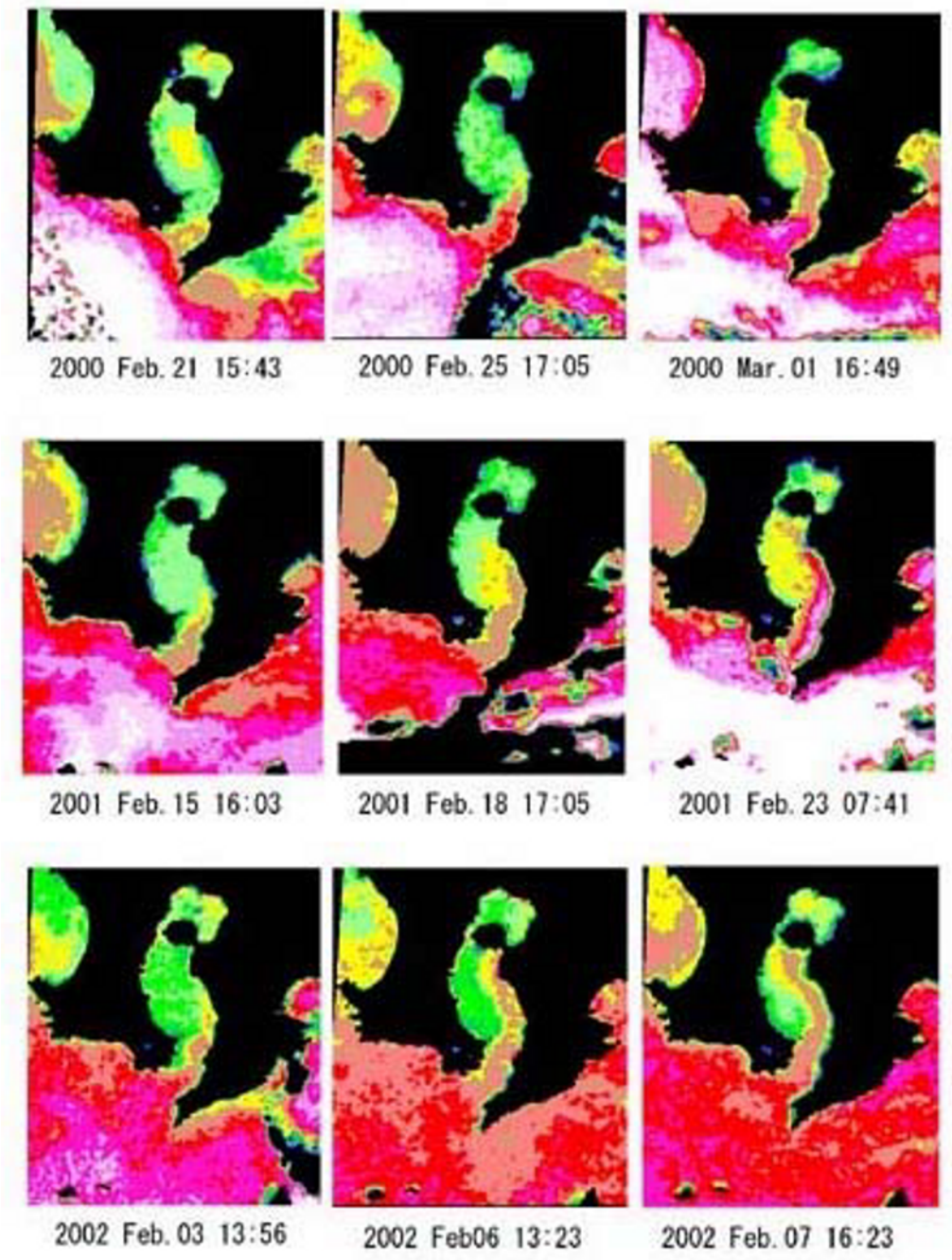

Fig. 5. Sea surface temperature images of NOAA/AVHRR.
Warm (cool) hues represent warm (cool) water.

3. Method of Numerical Simulation

Kubokawa and Hanawa (1984) investigated the intrusion of a density current along a coast in a rotating fluid. The theoretical model proposed is the shock wave solution of a semigeostrophic gravity wave in a shallow water equation. They concluded that once the warm water touches the bay water, it begins to intrude into the bay. The intrusion keeps the coast to the right in Northern Hemisphere owing to Coriolis' force as shown in Fig.6.

This section presents methods of a numerical simulation carried out for the purpose to investigate a coastal boundary current associated with the intrusion of warm water into the bay. The governing equations are given in the following:

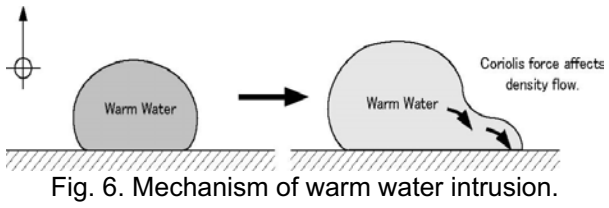

Fig. 6. Mechanism of warm water intrusion.

$$\frac{\partial u}{\partial t}+u\frac{\partial u}{\partial x}+v\frac{\partial u}{\partial y}+w\frac{\partial u}{\partial z}-fv=-\frac{1}{\rho}\frac{\partial P}{\partial x}+\frac{\partial}{\partial x}\left(\nu_H\frac{\partial u}{\partial x}\right)+\frac{\partial}{\partial y}\left(\nu_H\frac{\partial u}{\partial y}\right)+\frac{\partial}{\partial z}\left(\nu_V\frac{\partial u}{\partial z}\right) \quad \cdots\cdots(1)$$

$$\frac{\partial v}{\partial t}+u\frac{\partial v}{\partial x}+v\frac{\partial v}{\partial y}+w\frac{\partial v}{\partial z}+fu=-\frac{1}{\rho}\frac{\partial P}{\partial y}+\frac{\partial}{\partial x}\left(\nu_H\frac{\partial v}{\partial x}\right)+\frac{\partial}{\partial y}\left(\nu_H\frac{\partial v}{\partial y}\right)+\frac{\partial}{\partial z}\left(\nu_V\frac{\partial v}{\partial z}\right) \quad \cdots\cdots(2)$$

$$\frac{\partial u}{\partial x}+\frac{\partial v}{\partial y}+\frac{\partial w}{\partial z}=0 \quad \cdots\cdots(3)$$

$$\frac{\partial T}{\partial t}+\frac{\partial}{\partial x}(uT)+\frac{\partial}{\partial y}(vT)+\frac{\partial}{\partial z}(wT)=\frac{\partial}{\partial x}\left(K_H\frac{\partial T}{\partial x}\right)+\frac{\partial}{\partial y}\left(K_H\frac{\partial T}{\partial y}\right)+\frac{\partial}{\partial z}\left(K_V\frac{\partial T}{\partial z}\right) \quad \cdots\cdots(4)$$

$$-\frac{1}{\rho}\frac{\partial P}{\partial z}=g \quad \cdots\cdots(5)$$

$$\frac{\partial \zeta}{\partial t}-\frac{\partial}{\partial x}\left(\int_{-H}^{\zeta}u\,dz\right)-\frac{\partial}{\partial y}\left(\int_{-H}^{\zeta}v\,dz\right)=0 \quad \cdots\cdots(6)$$

where $u(v)$ is the longitudinal (latitudinal) velocity, w is the vertical velocity, f is the Coriolis' parameter, P is the pressure, g is the gravitational acceleration, ρ is the water density, $\nu_H(\nu_V)$ is the horizontal (vertical) eddy viscosity, $K_H(K_V)$ is the horizontal (vertical) diffusion constant, and T is the water temperature.

The simulation model in this paper employed the three-dimensional finite difference method (Multi-level model) applied to the density current. The basic assumptions of the method are the following:

1) Hydrostatic approximation for the vertical momentum equation.
2) Boussinesq's approximation.
3) f-plane approximation.

This paper is based on an assumption that the Kuroshio warm filament brings a warm water mass near the mouth of the bay. The calculations are performed in the following two cases.

Case 1: The thermal boundary condition.

Case 2: The thermal and the tidal boundary conditions.

Case 1 treats only the thermal density current. On the other hand, Case 2 treats not only the thermal effect but also the tidal effect.

The division of Kagoshima Bay by the square mesh elements is given in Fig. 7. The mesh size and the calculation parameters are given in Table 1. Table 2 shows the open boundary conditions for the above two cases.

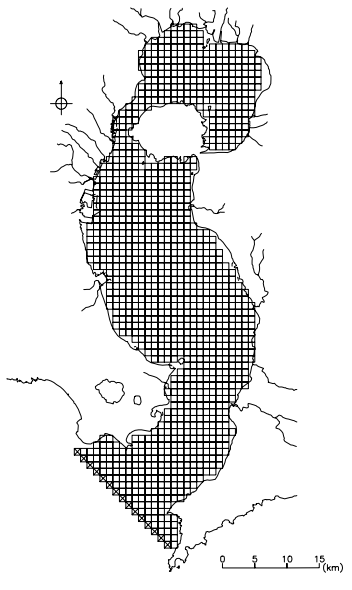

Fig. 7. Division of Kagoshima Bay.

The buoy robot observation indicates the warm water mass exists deeper than 10m. Then, the warm mass layer of 21℃ is chosen to be 20m in depth and assumed to touch to the mouth of the bay for two days. Only Semi-diurnal tide level is forced at the mouth of the bay, because it is outstanding in Kagoshima bay. The time series of the warm water mass layer and the tide level given at the open boundary are explained in Fig. 8.

Table 1. Mesh size and the calculation parameters.

Horizontal mesh size	$\Delta X,\Delta Y$	1.0km(Fig. 7)	
Level	ΔZ	10Layer	
		1:0m(surface)-10m	6:80m-100m
		2:10m-20m	7:100m-120m
		3:20m-40m	8:120m-140m
		4:40m-60m	9:140m-180m
		5:60m-80m	10:180m-bottom
Horizontal eddy viscosity constant	ν_H	1.0×10^5cm²/s	
Vertical eddy viscosity constant	ν_V	1.0×10^0cm²/s	
Horizontal diffusion ratio constant	K_H	0cm²/s	
Vertical diffusion constant	K_V	1.0×10^0cm²/s	
Coriolis parameter	f	8.0×10^{-5}s^{-1}	

Table 2. Open boundary conditions of the water temperature and the tide levels for the two cases.

Case 1	Temperature	0m-20m (Layer 1-2)	Initially uniformed (17℃). 21℃ given for two days, then uniformed (17℃) again.
		20m-Bottom	Uniformed (17℃)
	Salinity	Uniformed(34‰)	
	Elevation	Uniformed (0cm)	
Case 2	Temperature	0m-20m (Layer 1-2)	Initially uniformed (17℃). 21℃ given for two days, then uniformed (17℃) again.
		20m-Bottom	Uniformed (17℃)
	Salinity	Uniformed (34‰)	
	Elevation	Amplitude: 0.75m, Period: Semi-diurnal	

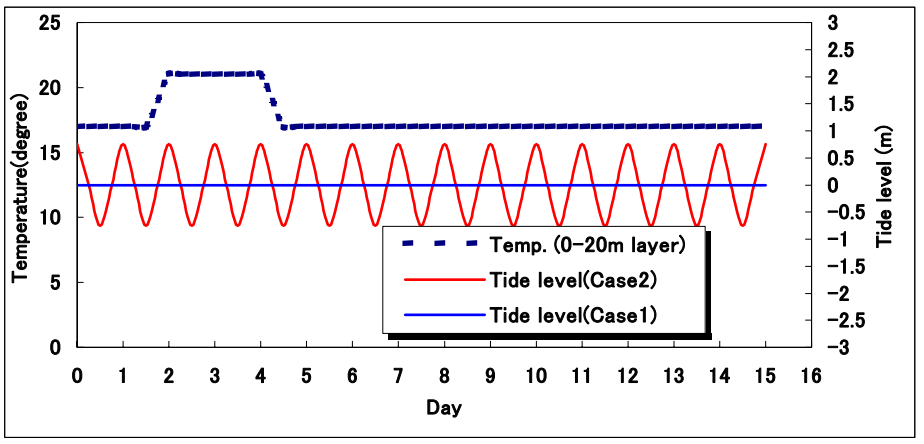

Fig. 8. Open boundary conditions for 15 days. The water temperature is ascended from 17°C to 21°C for two days.

4. Results

4.1 Sea Surface Temperature and Velocity Distributions

Figure 9.1 and 9.2 show the calculated sea surface temperature distributions up to 13th day in Case 1 and Case 2 boundary condition. In both cases, the warm water mass intrudes into the bay along the east coast. Even after the 5th day, when the water temperature at the open boundary goes back to the initial 17℃, the warm water mass continues to intrude into the bay.

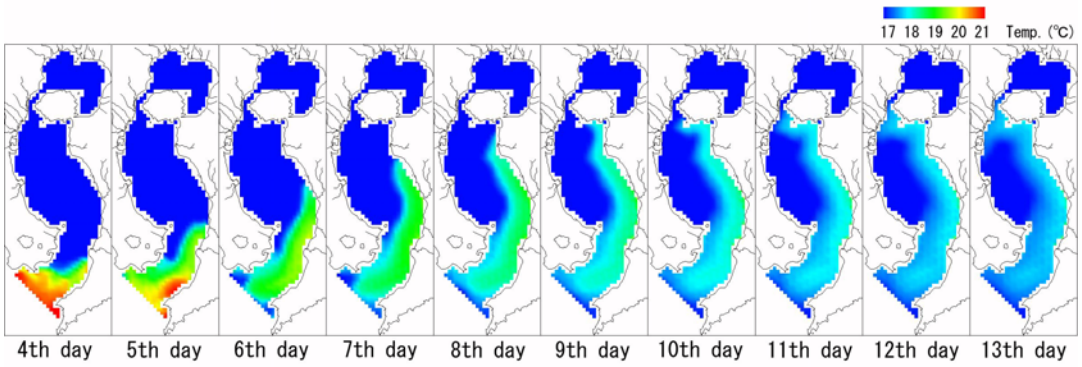

Fig. 9.1. Calculated surface temperature distributions for 13 days (Case 1).

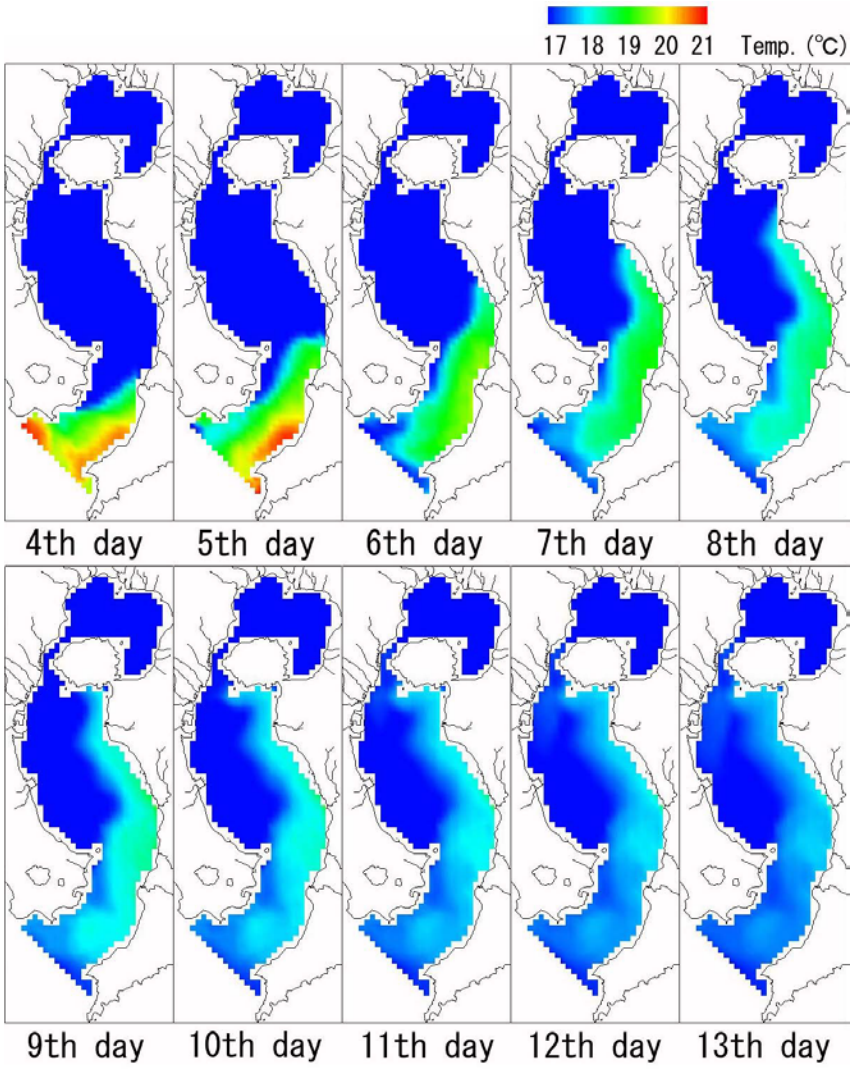

Fig. 9.2. Calculated surface temperature distributions for 13 days (Case 2).

At the 9th day, the warm water reaches at the southern coast of Sakurajima and begins to rotate anticlockwise. The difference between Case 1 and Case 2 is not so conspicuous. The tidal effects appear only around off Ibusuki and the southern area of Sakurajima Channel.

Figure 10.1 and 10.2 show the velocity distributions at the surface layer up to 12th day in Case 1 and Case 2 boundary condition. In both cases, calculated velocity at the 8th day is about 15cm/s near the leading head of the warm water mass and about 10cm/s around its middle. These velocities are similar to the results estimated from the buoy robot observations (Ohtani et al., 1998)

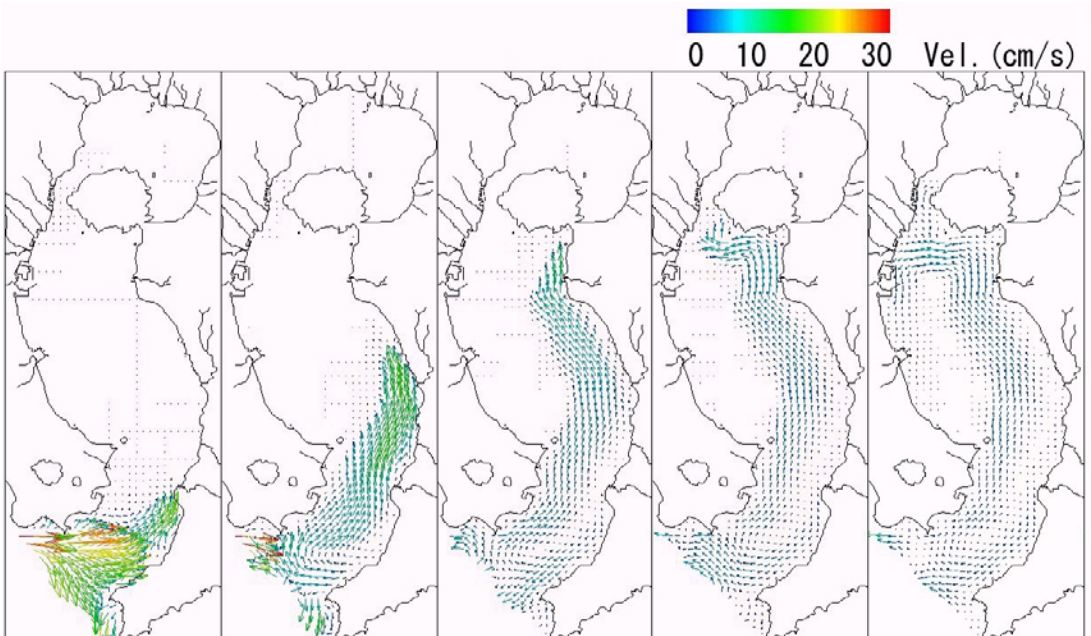

Fig. 10.1. Calculated current distributions for 12 days (Case 1).

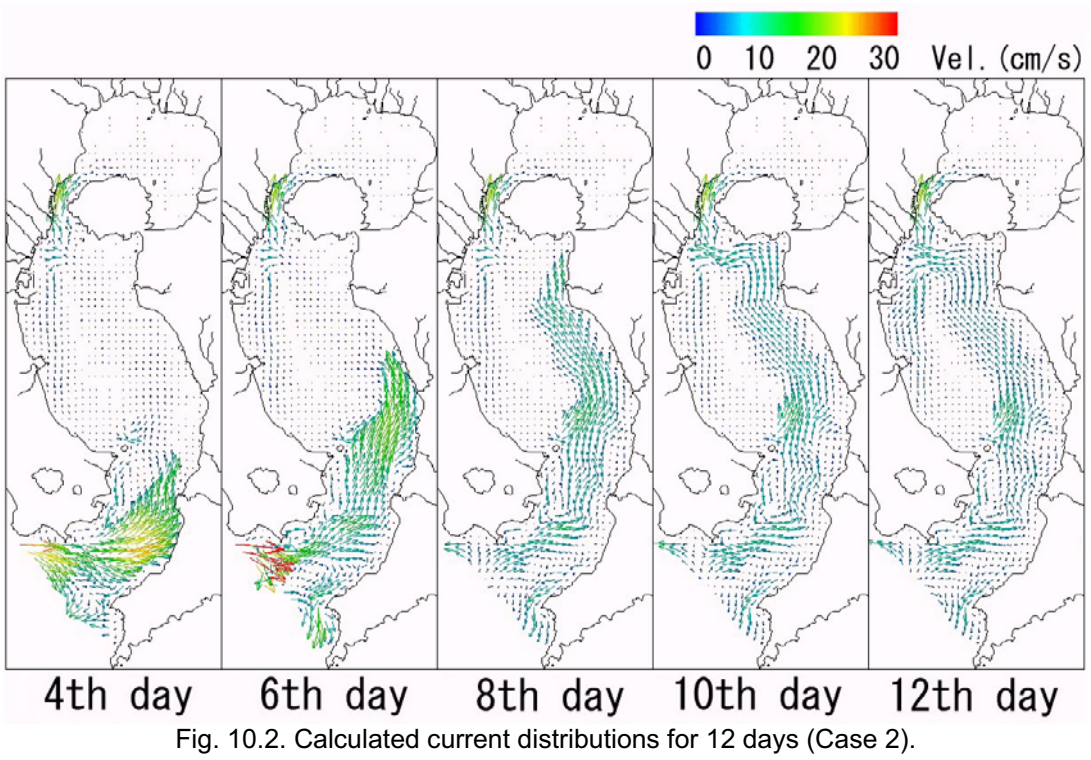

Fig. 10.2. Calculated current distributions for 12 days (Case 2).

and the NOAA images in Fig. 5. The tidal effects turn up especially in the southern flow along the west coast at the south of Sakurajima Channel and in the anticlockwise vortex off Ibusuki.

Since the tidal effect is not taken into account in Case 1 calculation, the anticlockwise rotation of the warm water at the south of Sakurajima Channel is not reproduced clearly. Even in Case 2 simulation, where the tidal effect is accounted, the anticlockwise rotation seems to be too close to the west coast. This incompatibility might be caused by the unsuitable fluid characteristics, e.g. the horizontal diffusion constant K_H set to be $0cm^2/s$ to represent the density difference near the open ocean.

The hydrostatic approximation adopted in our calculation might be improper especially at the leading head of the intruding warm water (Kubokawa and Hanawa, 1984). Nevertheless, the distribution of the calculated warm water mass up to 8th day is similar in form to the satellite images. In particular, the meandering of the surface temperature distribution from the open boundary to Kaigata is reproduced, especially in Case 2 calculation. After 8th day, the calculated temperature distributions resemble to Fig. 4b and Fig. 5, where the warm water reaches the southern coast of Sakurajima (first pattern). However, the image of Fig. 4c is not reproduced in our simulation. In Fig. 4c, the warm water does not reach to the southern coast of Sakurajima, but turns anticlockwise after arriving off Kanoya (second pattern). As there exist also some NOAA images similar to Fig. 4c, the warm water distribution pattern could be classified according to the beginning point of the anticlockwise rotation. In our present simulation, only the first pattern is reproduced and the cause of the second pattern remains for the future investigation.

4.2 Depth of Warm Water Mass

Figure 11 denotes the isothermal surface distributions of 17.5℃, which are detached from the coast denoted by red thin lines. It is seen from the figure, that the isothermal surface of 17.5℃ keeps the depth of about 20m during intruding and its distributions are almost the same as those of surface water intrusion in Fig. 9.2 except the areas close to the coast.

After 12th day, in the Case 1 calculation without tide (Fig. 11.1), the isothermal surface of 17.5℃ reaches the west coast, while in Case 2 (Fig. 11.2) it disappeared at the south of Sakurajima Channel.

5. Conclusion

The intrusion of the warm water into Kagoshima Bay in winter is frequently observed by the thermal infrared satellite images. The intrusion is considered to occur, when the Kuroshio warm filament comes into touch with the bay water (Akiyama, 1994). The effect of the warm water might spread to all over the south basin and will influence the exchange of the bay water and its water quality.

In this paper, we have simulated the intrusion of the warm water into the bay by the 10-leveled model of FDM. It is shown that the warm water begins to intrude into the bay, when it arrived at the mouth of the bay, in accord with Kubokawa and Hanawa (1984). The intrusion occurs regardless of tide. The tidal effects in the warm water distribution are only remarked at the south of Sakurajima Channel and off Ibusuki.

The present numerical calculation is carried out based on many assumptions, particularly the thickness of the warm water at the open boundary is assumed to be 20m and the horizontal diffusion constant is zero. We have reproduced only one of the two patterns of the warm water distribution in winter. It is important to investigate in which condition the second pattern appears.

As far as looking over the results of calculation, the unstructured cross grids do not lead to any serious problem. However, the cross grids might affect to the tidal velocity especially at narrow Sakurajima Channel and at the mouth of the bay, where the boundary condition is forced. The calculation using FEM is now in progress.

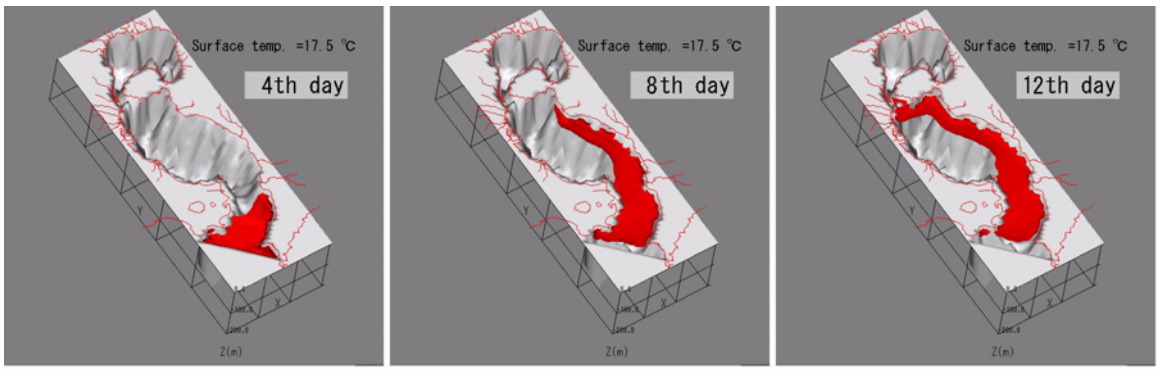

Fig. 11.1. Calculated isothermal surface distributions of 17.5°C (Case 1).

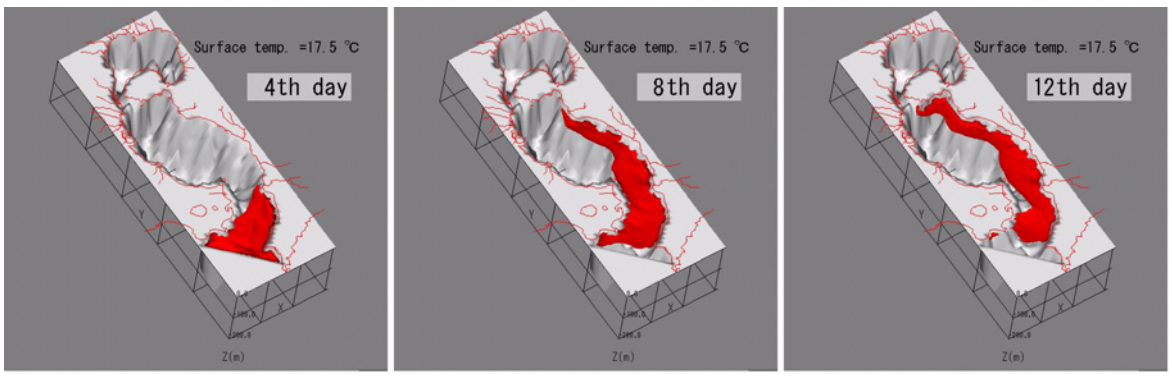

Fig. 11.2. Calculated isothermal surface distributions of 17.5°C (Case 2).

We have only enforced Semi-diurnal (M2) tide level at the mouth of the bay. If other harmonic tidal components, e.g. S2, K1, O1, are included, the spring and the neap tides appear. For the purpose to compare a satellite image to a calculated result, the effect of other harmonic components as well as wind stress should be taken into account. However, the aim of this paper is to investigate the mechanism of warm water intrusion into a bay. The quantitative comparison of observed and calculated patterns is left for future work.

We have calculated the ocean water intrusion into the bay only in winter, when the temperature and the salinity could be assumed to be almost uniform in all over the bay. There is no observation to know whether the ocean water intrusion occurs in other seasons or not. The numerical simulation could be also helpful for this problem.

References

Akiyama, H., The Movement of the Warm Water Filament Appeared at the South and East Oceans of Kyusyu, Monthly Ocean Magazine, 26 (1994), 689-697 (in Japanese).

Kikukawa, H., Harashima, A., Hama, K. and Matsuzaki, A., A Numerical Study of the Seasonal Differences of Circulation Processes in a Nearly Closed Coastal Basin, Estuarine, Coastal and Shelf Science, 44 (1997), 557-567.

Kubokawa, A. and Hanawa, K., A Theory of Semigeostrophic Gravity Waves and its Application to the Intrusion of a Density Current along a Coast, Part 1. Semigeostrophic Gravity Waves, Journal of the Oceanographical Society of Japan, 40 (1984), 247-259.

Kubokawa, A. and Hanawa, K., A Theory of Semigeostrophic Gravity Waves and its Application to the Intrusion of a Density Current along a Coast, Part 2. Intrusion of a Density Current along a Coast in a Rotating Fluid, Journal of the Oceanographical Society of Japan, 40 (1984), 260-270.

Ohtani, M., Kikukawa, H., Orita, K., Kohno, J. and Kinoshita, K., Ocean Water Inflow into Kagoshima Bay, Umi no Kenkyu, 7 (1998), 245-251 (in Japanese).

Sakurai, M., Water Exchange through the Mouth of Kagoshima Bay, Bulletin on Coastal Oceanography, 21 (1983), 45-52 (in Japanese).

Takahashi, T., Seasonal Differences of the Circulation Processes in a Coastal Basin Nearly Closed by Land, Ocean Management, 6 (1981), 189-200.

Author Profile

Jun-ichi Kohno: He received his B.Sc. (1976) and his Ph.D. (1984) in Physics from Kyushu University. From 1993, he serves as a researcher for Kagoshima Environmental Research and Service. His research interests are environmental fluid dynamics and satellite remote sensing.

Kazunori Hosotani: He received his B.Eng.(1996) and M.Eng.(1999) in Mechanical engineering from Tottori University. After B.Eng., he worked in the CKD Co., Ltd. Since 1999, he is currently an engineer at the Kagoshima Environmental Research and Service. His research interest is environmental fluid dynamics.

Yuhsaku Ono: He received his B.Fish. (2003) from Kagoshima University. He is a student of Master course in the Faculty of Fisheries of Kagoshima University. His research interest is satellite remote sensing on the coastal environment.

Hiroyuki Kikukawa: He received his B.Sc. (1967) and his Ph.D. (1973) in Physics from University of Tokyo. After Ph.D., he works at Kagoshima University (1974-) in the field of coastal oceanography. He is a professor of Kagoshima University. His research interests are satellite remote sensing and numerical study on the coastal environment.